17. 5. 2004 BI-TP 2004/11

The SPS Heavy Ion Programme

Helmut Satz

Fakultät für Physik, Universität Bielefeld
Postfach 100 131, D-33501 Bielefeld, Germany
and
Centro de Física das Interacções Fundamentais (CFIF)
Instituto Superior Técnico, P-1049-001 Lisbon, Portugal

States of Matter in QCD

During the past fifty years, our concept of an elementary particle has undergone a fundamental change. Today we understand hadrons as bound states of quarks, and thus as composite. In strong interaction physics, quarks have become the smallest building blocks of nature. But the binding force between quarks confines them to their hadron, which cannot be split into its quark constituents. In terms of individual existence, hadrons remain elementary.

This modification of our hadron picture has led to remarkable consequences in strong interaction thermodynamics: at high temperature or density, hadronic matter must become a plasma of deconfined quarks and gluons. In return, strong interaction thermodynamics points out the limits of quark confinement: in a sufficiently hot or dense medium, quarks can become free.

Such high densities prevailed in the very early universe, until some 10^{-5} seconds after the big bang; only then were quarks confined to form hadrons. To create and study this primordial plasma in the laboratory is one of the great challenges for current experimental physics. Various estimates indicate that the collision of two heavy nuclei at very high energy might indeed produce short-lived bubbles of deconfined matter. CERN has played a vital role in initiating the experimental use of heavy ion collisions to search for the quark-gluon plasma, and it has in the past two decades provided fundamental contributions which today form the basis of our present understanding of the field.

Conceptually, the thermodynamics of strongly interacting matter leads to three forms of critical behaviour.

- In QCD, hadrons are dimensionful colour-neutral bound states of pointlike coloured quarks and gluons. Hadronic matter, consisting of colourless constituents of hadronic dimension, can therefore turn into a quark-gluon plasma of pointlike coloured quarks and gluons. This deconfinement transition is the QCD counterpart of the insulator-conductor transition in atomic matter.
- In vacuum, quarks dress themselves with gluons to form the constituent quarks that make up hadrons. As a result, the bare quark mass $m_q \sim 0$ is replaced by a constituent quark mass $M_q \sim 300$ MeV. In a hot medium, this dressing melts and $M_q \to 0$. Since the QCD Lagrangian for $m_q = 0$ is chirally symmetric, $M_q \neq 0$ implies spontaneous chiral symmetry breaking. The quark mass shift $M_q \to 0$ thus corresponds to chiral symmetry restoration.

- A third type of transition would set in if the attractive interaction between quarks in the deconfined phase produces coloured bosonic diquarks, the Cooper pairs of QCD. These diquarks can then condense at low temperature to form a colour superconductor. Heating will dissociate the diquark pairs and turn the colour superconductor into a normal colour conductor, the quark-gluon plasma.

With the baryochemical potential μ as a measure for the baryon density of the system, we thus expect the phase diagram of QCD to have the schematic form shown in Fig. 1.

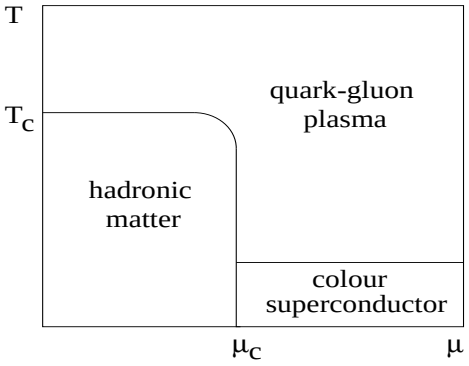

Figure 1: Phase diagram of QCD

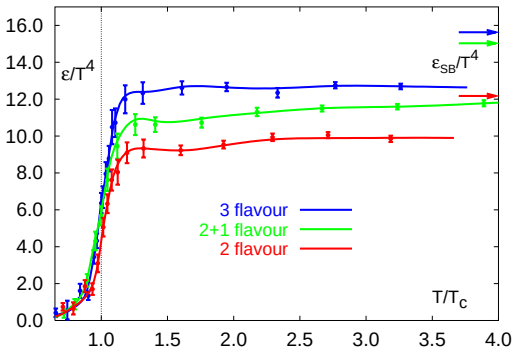

Figure 2: Energy density in QCD

Based on the QCD Lagrangian as dynamics input, the thermodynamics of strongly interacting matter is in principle fully specified, and at least for vanishing overall baryon density, finite temperature lattice QCD provides today quite detailed predictions [1]. We here briefly summarize the most important features.

The energy density of an ideal gas of massless pions is

$$\epsilon_h = 3\frac{\pi^2}{30}T^4 \simeq T^4, \tag{1}$$

while an ideal gas of massless quarks (for $N_f = 2$) and gluons gives

$$\epsilon_q = 37\frac{\pi^2}{30}T^4 \simeq 12\ T^4. \tag{2}$$

Deconfinement thus produces a sudden increase in energy density, corresponding to the latent heat of deconfinement [2]. This behaviour is in fact found in lattice QCD [3], as shown in Fig. 2. For two light quark species, as well as for two light and one heavy species, the transition temperature becomes $T_c \simeq 175\pm15$ MeV, and the resulting energy density at deconfinement becomes $\epsilon(T_c) \simeq 0.3-1.3$ GeV/fm^3. The abrupt change of behaviour of the energy density can be related directly to deconfinement and chiral symmetry restoration.

Deconfinement is specified by the Polyakov loop expectation value [4]

$$L \sim \exp\{-F_{Q\bar{Q}}/T\} \tag{3}$$

where $F_{Q\bar{Q}}$ denotes the free energy of a $Q\bar{Q}$ pair in the limit of infinite separation. In the confinement regime, $F_{Q\bar{Q}}$ diverges and hence $L = 0$; in a deconfined medium, colour

screening makes the free energy finite and hence $L \neq 0$. Thus the change of behaviour of L defines the deconfinement temperature T_L.

Chiral symmetry restoration is determined by the chiral condensate $\langle\bar{\psi}\psi\rangle \sim M_q$, which measures the dynamically generated constituent quark mass M_q. When $\langle\bar{\psi}\psi\rangle \neq 0$, the chiral symmetry of the Lagrangian is spontaneously broken, and when $\langle\bar{\psi}\psi\rangle = 0$, it is restored. Hence the change of behaviour of $\langle\bar{\psi}\psi\rangle$ defines the chiral symmetry restoration point T_χ.

In detailed lattice studies [5] it is shown that the two transitions clearly occur at the same temperature: at $\mu = 0$, chiral symmetry restoration and deconfinement coincide. We can thus conclude that QCD predicts for $\mu = 0$ one thermal transition from hadronic matter to a quark-gluon plasma. For $N_f = 2$ or 2+1, it occurs at $T_c \simeq 175$ MeV; at this temperature, chiral symmetry is restored, deconfinement sets in, and the energy density increases quite suddenly by the "latent heat" of deconfinement.

The nature of the transition has been a subject of much attention by theorists, but so far, it is not fully clarified, since it depends quite sensitively on the baryon density as well as on N_f and m_q. For a theory with one heavier and two light quarks, one expects [6] non-singular behaviour (rapid cross-over, perhaps percolation) in a region between $0 \leq \mu < \mu_t$, a critical point at μ_t, and beyond this a first order transition (see Fig. 3). Recent lattice calculations in a theory with two quarks of finite mass provide some support for such behaviour; as shown in Fig. 4, the baryon density fluctuations develop a pronounced peak with increasing baryochemical potential, which might indicate the approach to a nearby critical point [7].

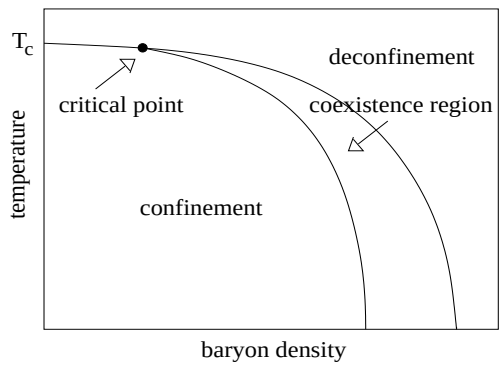

Figure 3: Phase diagram as function of baryon density

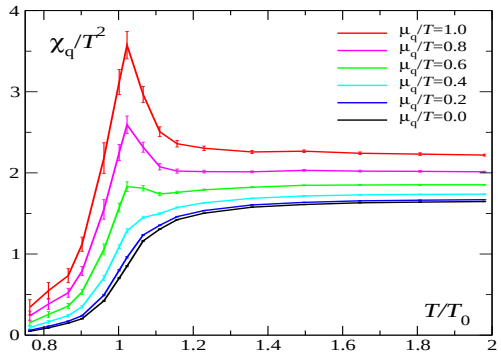

Figure 4: Baryon susceptibility χ_q vs. temperature

High Energy Nuclear Collisions

The heavy ion programme at the CERN-SPS was created with the aim to produce the quark-gluon plasma in the laboratory and to study both the deconfinement transition and the new deconfined state of matter. Starting from the non-equilibrium configuration of the two colliding nuclei, the evolution of the collision was assumed to have the form illustrated in Fig. 5. After the collision, there is a short pre-equilibrium stage, in which the primary partons of the colliding nuclei interact, multiply and then thermalize to form a quark-gluon plasma. This then expands, cools and hadronizes.

In recent years, the effect of pre-equilibrium conditions on deconfinement have been studied in more detail; in particular, it now appears conceivable that nuclear collisions lead to a specific form of deconfinement without ever producing a thermalized plasma of quarks and gluons. We shall return to these aspects later and here address first the probes proposed to study the different stages and properties of a thermal medium.

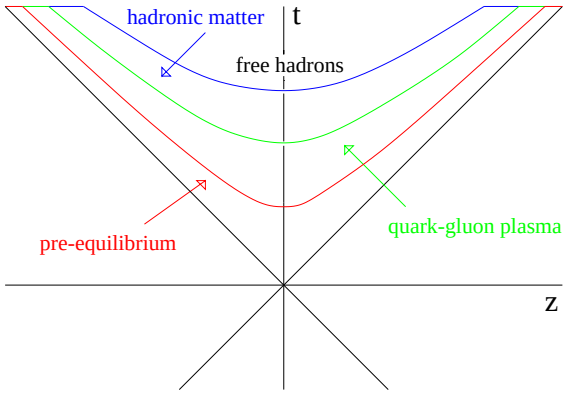

Figure 5: Expected evolution of a nuclear collision

The initial energy density of the produced medium at the time of thermalization was estimated by [8]

$$\epsilon = \left(\frac{dN_h}{dy}\right)_{y=0} \frac{w_h}{\pi R_A^2 \tau_0}, \tag{4}$$

where $(dN_h/dy)_{y=0}$ specifies the number of hadrons emitted per unit rapidity at mid-rapidity and w_h their average energy. The initial volume is determined in the transverse nuclear size (radius R_A) and the formation time $\tau_0 \simeq 1$ fm of the thermal medium.

The determination of the nature of the hot initial phase required deconfinement signatures. It was argued that in a hot quark-gluon plasma, the J/ψ would melt through colour screening [11], so that QGP formation should lead to a suppression of J/ψ production in nuclear collisions. Similarly, the QGP was expected to result in a higher energy loss for a fast passing colour charge than a hadronic medium, so that increased jet quenching [12] should also signal deconfinement.

The temperature of the produced medium, in the confined as well as in the deconfined phase, was assumed to be observable through the mass spectrum of thermal dileptons and the momentum spectrum of thermal photons [9, 10]. The observation of thermal dilepton/photon spectra would also indicate that the medium was indeed in thermal equilibrium.

The behaviour of sufficiently short-lived resonances, in particular the dilepton decay of the ρ, was considered as a viable tool to study the hadronic medium in its interacting stage and thus provide information on the approach to chiral symmetry restoration [13].

The expansion of the hot medium was thought to be measurable through broadening and azimuthal anisotropies of hadronic transverse momentum spectra (flow) [14]. The size and age of the source at freeze-out was assumed to be obtainable through Hanbury-Brown–Twiss (HBT) interferometry based on two-particle correlations [15]. It was expected that

Experiment	Observables	Probing
NA34/HELIOS2 HELIOS3	hadrons dimuons	hadron spectra in−medium hadron modifications
NA35/49	charged hadrons strange hadrons	hadron spectra, correlations, flow abundances, strangeness
NA36	strange hadrons	strangeness production
NA44	pions and kaons	HBT interferometry, spectra at y = 0
NA45/CERES	dielectrons charged hadrons	in−medium hadron modifications correlations
NA38/50 NA60	dimuons	J/ψ and Drell−Yan production χ_c and open charm production in − medium hadron modifications
NA52	low Z/A nuclei	strangelets
WA80/93/98	photons	thermal photons, pion spectra, flow
WA85/94/97, NA57	hyperons	strangeness enhancement

Table 1: Heavy ion experiments at the CERN-SPS

increasing the collision energy would increase the density and hence the expansion of the produced medium, so that the HBT radii should grow with increasing $\sqrt{s}$ [16].

The final interacting hadronic medium had been discussed in terms of an ideal resonance gas, which at vanishing overall baryon density would provide the relative abundances of all hadron species in terms of just one parameter, the limiting temperature of hadronic matter [17]. The species abundances in elementary hadronic interactions follow such a pattern [18], but with an overall reduction of strangeness production. Nuclear collisions, if leading to the formation of a hot quark-gluon plasma with a thermal density of strange quarks and antiquarks, were expected to remove this reduction and thus result in enhanced strangenes production in comparison to *pp* interactions [19]. – The formation of strange baryonic matter ('strangelets') was also considered [20].

In order to address the features just outlined, CERN started an extensive experimental programme, as summarized in Table 1. Since the ion injector available in 1986 was

restricted to nuclei with equal numbers of protons and neutrons, the initial programme used ^{16}O and ^{32}S beams of $P_{Lab}/A \simeq 200$ GeV/c on different heavy targets. Subsequently an injector was constructed to accommodate arbitrarily heavy nuclei; with its help, the use of ^{208}Pb beams with $P_{Lab}/A \simeq 160$ GeV/c started in 1995. We now summarize the main results obtained by the programme so far; one experiment (NA60) is continuing with ^{115}In beams at least up to the year 2005.

Experimental Results

The initial energy density, as specified by the Bjorken estimate, Eq. (4), was measured in almost all SPS experiments. In Fig. 6, we show ϵ as function of centrality, determined by the number of participant nucleons [21]; it covers the range from somewhat above 1 to almost 3.5 GeV/fm^3 and thus reaches well above the deconfinement value.

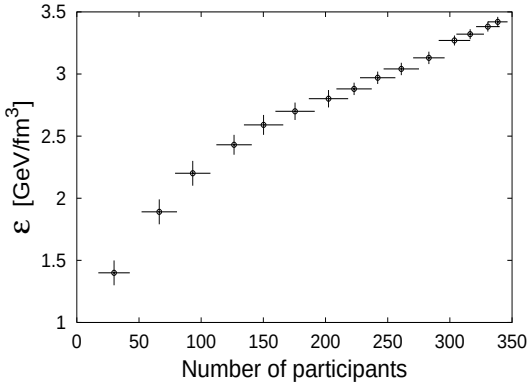

Figure 6: Energy density in Pb-Pb collisions [21].

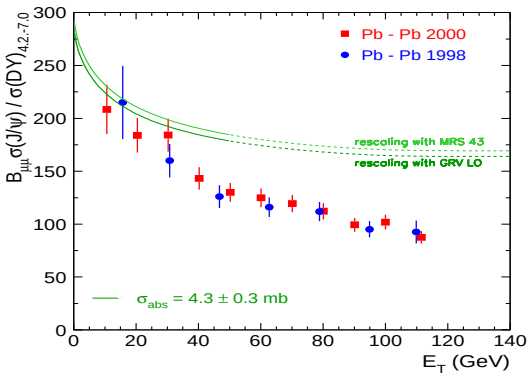

Figure 7: Ratio of J/ψ to Drell-Yan production in Pb-Pb collisions [21].

J/ψ production was found to be suppressed in O-U, S-U and then Pb-Pb collisions; the suppression always increases with centrality [22]. In p-A collisions, it was observed that already normal nuclear matter leads to reduced charmonium production. Extrapolating this 'normal' suppression to nucleus-nucleus interactions is enough to account for the observed yields up to central S-U collisions. Peripheral Pb-Pb collisions also follow the normal pattern; then, with increasing centrality, there is a pronounced onset of a further 'anomalous' suppression [21], as shown in Fig. 7.

In pp and pA collisions, the dilepton mass spectrum in the region around and below the ρ peak is well reproduced by the yield from known hadronic sources. In AA collisions, it was found to differ considerably from this expected yield [23, 24], indicating in-medium resonance modifications (Fig. 8). This 'low mass dilepton enhancement' is observed in S-U and Pb-Pb collisions, and for the latter at beam energies of 40 GeV as well as of 160 GeV [25].

Similarly, some photon excess over the expected normal hadronic decay yield has been reported [26], as well as an excess of dileptons in the mass range between the ϕ and the J/ψ [27].

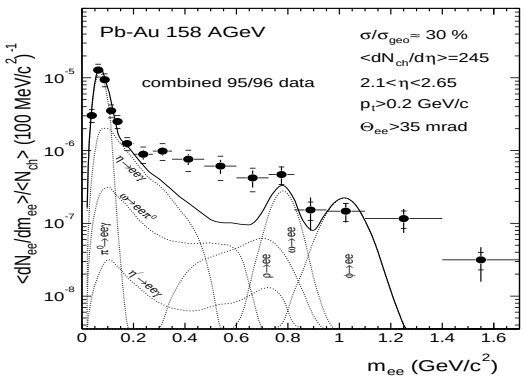

Figure 8: Dilepton production compared to the expected yield from known hadronic sources [23].

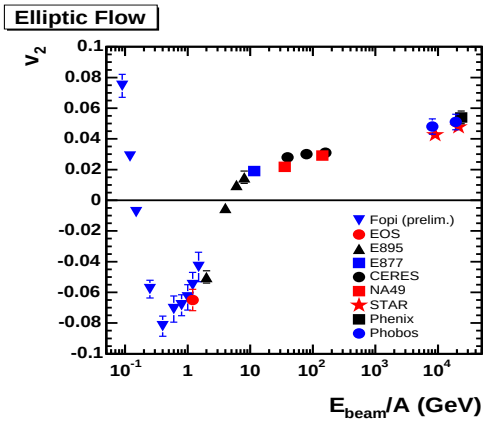

Figure 9: Elliptic flow at different beam energies [28].

The broadening of transverse momentum spectra, expected as consequence of transverse flow, was observed in the predicted form, increasing with increasing hadron mass. Moreover, transverse momentum spectra also showed the azimuthal anisotropy (elliptic flow) predicted for non-central collisions. The behaviour shown in Fig. 9 indicates that at low collision energy, production is reduced by the presence of spectator nucleons; at high energy, there is enhanced production in the direction of the higher pressure gradient as determined by the anisotropic interaction volume [28].

In HBT correlation studies it is found that at all energies the source radii are essentially determined by those of the involved nuclei [28]; the expected increasing source size was not observed. Thus one finds for the transverse radii $R_{\rm side} \simeq R_{\rm out} \simeq 5-6$ fm for Au-Au/Pb-Pb collisions from AGS to SPS and on to RHIC, as seen in Fig. 10. The approximate equality of $R_{\rm out}$ and $R_{\rm side}$ is another unexpected feature, since their difference should be a measure of the life-time of the emitting medium.

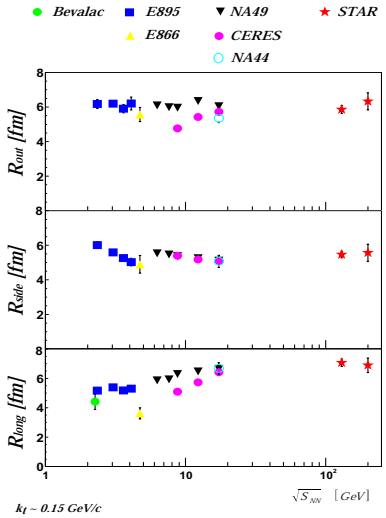

Figure 10: HBT radii at different beam energies [28].

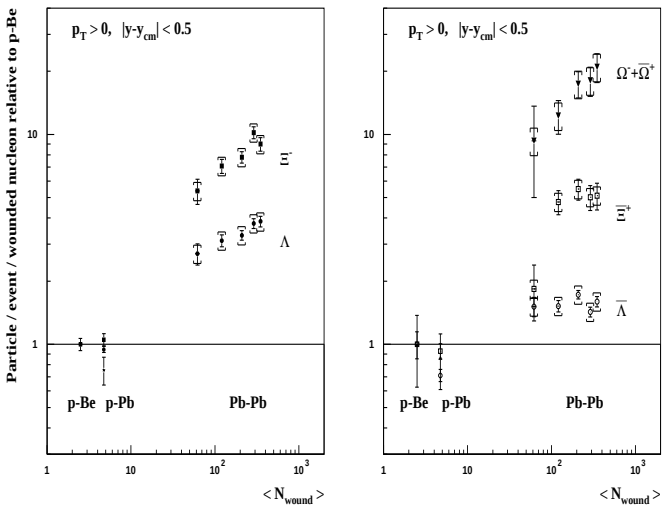

Figure 11: Hyperon production as function of centrality, normalized to p-Be results [29].

The expected enhancement of strangeness production was indeed observed; the ratio of strange to non-strange hadrons in AA collisions, compared to the same ratio in pp collisions, always increased significantly. In Fig. 11 we show the most striking example, in which the production of hyperons is increased up to 10 times and more in comparison to $p - Be$ rates [29]. – No indication for strangelet production was found [30]

Conclusions, Questions, Outlook

The wealth of experimental results obtained so far has clearly established that high energy nuclear interactions produce large-scale complex systems which show a number of specific collective effects and thus provide more than a superposition of independent nucleon-nucleon collisions. Let us see what conclusions the individual observations lead to.

The essential issues for the CERN heavy ion programme were:

- do the colliding nuclei produce a system of deconfined quarks and gluons,
- can the produced system be described in thermal terms,
- is there any rapid change of an observable, indicating critical behaviour.

The quark-gluon plasma of statistical QCD is a deconfined system in thermal equilibrium. However, as we shall see shortly, pre-equilibrium studies suggest that in nuclear collisions, deconfinement and thermalization should be addressed as two distinct issues.

Hard probes meant to test the nature of the early medium can suffer nuclear effects at different points in the evolution of the collision. The presence of a nuclear target can modify the production of the probe, as seen in pA collisions. Once formed, the probe can interact with the partons in the pre-equilibrium stage, and/or it can subsequently be effected by the QGP and the final hadronic medium. It is thus important to distinguish between initial nuclear effects from those due to different evolution stages of the medium formed by the collision.

The partonic constituents in the initial state of a high energy nuclear collision are given by the parton distribution function of the colliding nuclei. To produce a large-scale thermal system, partons from different nucleon-nucleon collisions have to undergo multiple interactions. In the center of mass initial state of a high energy collisions, the nuclei are strongly Lorentz contracted; the resulting parton distribution in the transverse collision plane is schematically illustrated in Fig. 12. The transverse size of the partons is determined by their intrinsic transverse momentum, and the number of partons contained in a nucleon is known from deep inelastic scattering experiments. The density of partons increases with both A and $\sqrt{s}$, and at some critical point, parton percolation occurs [31] and "global" colour connection sets in. In the resulting parton condensate, partons lose their independent existence and well-defined origin, so that this medium is deconfined, though not thermalized. In recent years, such partonic connectivity requirements (closely related to parton saturation) and the properties of a connected pre-thermal primary state (colour glass condensate) have attracted much attention [31, 32].

We thus have to determine if some specific observed behaviour is due to nuclear effects on the formation of the probe, to the parton condensate in the initial pre-equilibrium stage, or to the presence of a deconfined or confined thermal medium. The problem is particularly transparent in the case of J/ψ suppression.

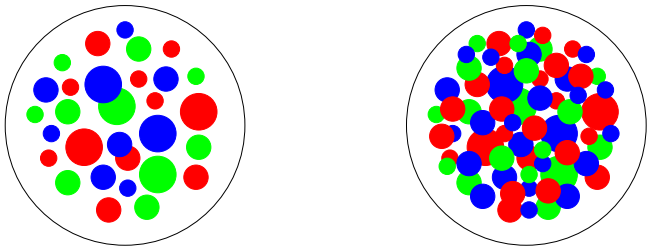

Figure 12: Parton distributions in the transverse plane of a nucleus-nucleus collision

As already mentioned, charmonium production in pA collisions is reduced in comparison to that in pp collisions, so that the presence of the nuclear target modifies the production of the probe. Once this 'normal' suppression, shown by the solid line in Fig. 7, is taken into account, any further 'anomalous' suppression, as seen in central $Pb-Pb$ collisions, is then due to the presence of a produced medium.

J/ψ production in pp collisions has shown that only about 60% of the observed J/ψ's are produced directly as $1S$ $c\bar{c}$ states; the remainder comes from decay of the (larger) excited states χ_c and ψ'. Now the effect of any medium on a charmonium state depends on the intrinsic scales of medium and probe. It is today known from finite temperature lattice QCD [33] that in a QGP the higher excited states χ_c and ψ' are dissolved at approximately the deconfinement point, while the smaller ground state J/ψ survives up to significantly higher temperature. Present calculations give 1.5 - 2 T_c for the dissociation point, but do not yet allow calculations of the width of the state as function of temperature. In a similar fashion, a pre-equilibrium parton condensate with a given resolution scale can dissociate only charmonia it can resolve. Here it is also found that the larger excited states are suppressed at the overall onset of parton percolation, while the ground state survives up to higher parton densities [34]. In both cases we thus expect a two-step suppression pattern: first the χ_c and ψ' disappear, which suppresses the J/ψ's from their decay, later the directly produced ground state is suppressed. In contrast, any suppression in a hadronic medium leads to a smooth variation without threshold [35].

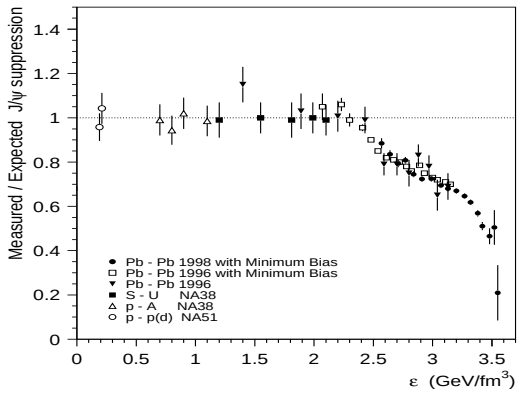

Figure 13: J/ψ suppression vs. energy density [21].

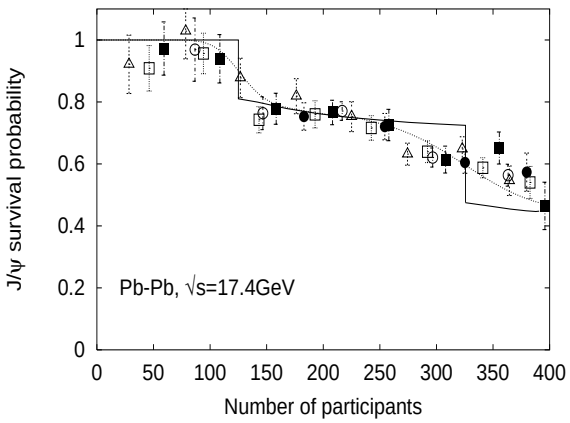

Figure 14: J/ψ suppression and parton condensation [34].

The NA50 data [21] indeed indicate a two-step pattern (see Fig. 7), although the second step is less pronounced and has also been attributed to multiplicity fluctuations in central

collisions [36]. Threshold energy density estimates, based on the Bjorken form (4) with $\tau_0 = 1$ fm, give around 2 - 2.5 GeV/fm^3 for the initial onset of anomalous suppression; as seen in Fig. 13, this does not agree with the lattice QCD result for deconfinement, $\epsilon(T_c) \simeq 0.3 - 1.3$ GeV/fm^3. In contrast, the parton percolation threshold ($N_{\rm part} \simeq 125$) agrees well with the first step of the anomalous J/ψ suppression (see Fig. 14), removing χ_c and ψ' contributions; the second step is compatible with percolation of harder partons [34]. Evidently the relevant variable for the threshold points is crucial, and this can be corroborated by experiments at different A or $\sqrt{s}$, since both enter in the parton density. Further confirmation and clarification of the threshold behaviour in J/ψ suppression is of decisive importance. It is the only clear onset of new behaviour, and hence the only indication for any form of critical behavior seen in any heavy ion experiment, and it can only be accounted for in terms of deconfinement. For this there are two distinct possibilities: parton percolation in the pre-equilibrium stage, or colour screening in a thermalized stage. The final conclusion must necessarily come from experiment.

All other phenomena studied at the SPS arise in the hadronic stage of the collision evolution and can thus be used to study the medium at the hadronization transition and later on. Here the issue of thermal behaviour is of fundamental importance, since from our pre-hadronic information it is so far not at all obvious that the collision of two heavy nuclei will produce systems which can be understood in terms of equilibrium thermodynamics. There are several observations which confirm that in the hadronic stage this is indeed the case.

The partonic cascades produced by elementary hadron-hadron collision (or by e^+e^- annihilation) evolve in space and time, eventually reaching a scale that requires hadronization. This transformation is known to lead to hadron abundances (for up to 30 different species) as given by an ideal resonance gas of a universal hadronization temperature T_h [18]; see Fig. 15. The hadronization temperature T_h has been determined for elementary collisions at a variety of different collision energies (Fig. 16). It agrees well with that predicted for the QCD confinement transition (the line T_c in Fig. 16), so that apparently the transition from partonic to hadronic degrees of freedom in such a system is in accord with statistical QCD. Since in the elementary collisions at the indicated $\sqrt{s}$, neither energy nor parton densities are high enough for any kind of deconfinement, the observed thermal abundance pattern is apparently not due to the formation of a deconfined medium in the pre-hadronization stage.

In central AA collisions, nuclear stopping leads at AGS and SPS energies to a medium of a much higher baryon density than that formed in corresponding pp interactions at mid-rapidity. Nuclear stopping is very much $\sqrt{s}$-dependent, which permits changes in the effective baryon density of the system under study. The basic question is whether the species abundances in AA collisions are still those of an ideal resonance gas, with thermal parameters which register baryon density changes of the medium, both as function of $\sqrt{s}$ and in comparison to pp. The answer is clearly affirmative [37]; we concentrate on central AA collisions and always consider mid-rapidity, to avoid averaging over different baryon densities.

- From SIS to RHIC, the species abundances in AA collisions are given by an ideal resonance gas, specified by a hadronization temperature T and a baryochemical potential μ; in Fig. 17 we show the behaviour at the top SPS energy [38]. The resulting 'freeze-out curve' in the T, μ plane is shown in Fig. 18 [39].

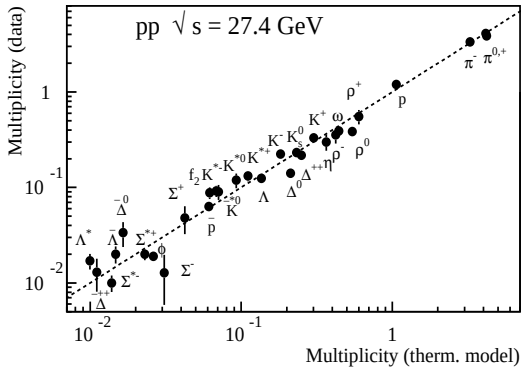

Figure 15: Thermal hadronization in pp collisions, $T = 175$ MeV [18].

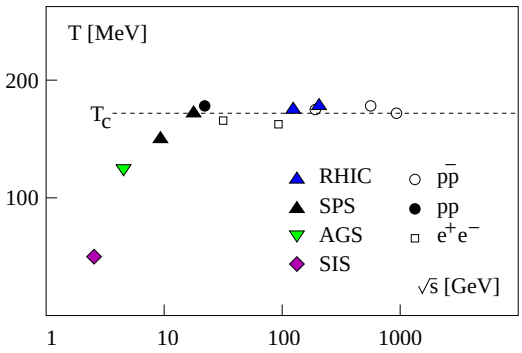

Figure 16: Thermal hadronization temperatures.

- The baryon density in AA collisions vanishes in the limit of high collision energy ('nuclear transparency'), so that $\mu \to 0$ for $\sqrt{s} \to \infty$. The corresponding T_h should therefore approach the deconfinement transition temperature T_c, as it does in high energy elementary collisions. In Fig. 16 it is seen that this is the case.
- For $\mu \neq 0$, the interacting hadron gas formed at the confinement transition contains non-resonant baryon repulsion and therefore cannot be approximated as an ideal resonance gas [40]. Hence for $\mu \neq 0$, the freeze-out curve no longer coincides with the deconfinement curve, as indicated in Fig. 18.
- The baryon density $n_B(\sqrt{s})$ along the freeze-out curve is shown in Fig. 19a. With increasing $\sqrt{s}$, the two nuclei penetrate each other more and more, so that the baryon density increases. Around $\sqrt{s} \simeq 7$ GeV, the nuclei begin to pass through each other, nuclear transparency sets in, and n_B starts to decrease.

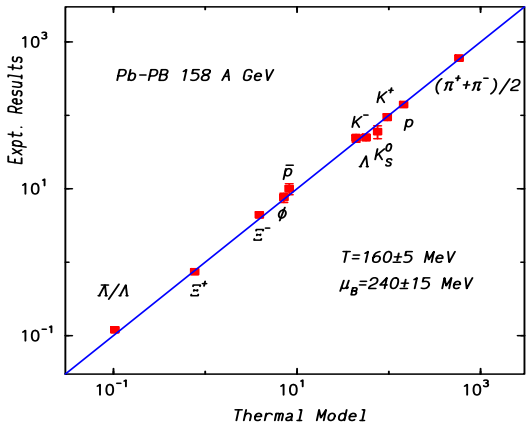

Figure 17: Hadron abundances in Pb-Pb collisions [38].

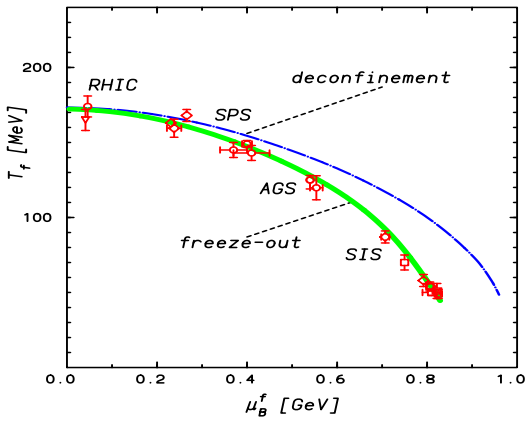

Figure 18: Freeze-out [39].

Thus nuclear stopping leads to a very characteristic $\sqrt{s}$-dependence of the baryon density along the freeze-out curve. Since the associated production of strange particles increases with increasing baryon density, this behaviour is reflected in the ratios K^+/π^+ and Λ/π,

as illustrated in Figs. 19b and c [41]. They are 'enhanced' at finite n_B, and when $n_B \to 0$, they decreases to the finite value given by the resonance gas at $T = T_h,\ \mu = 0$.

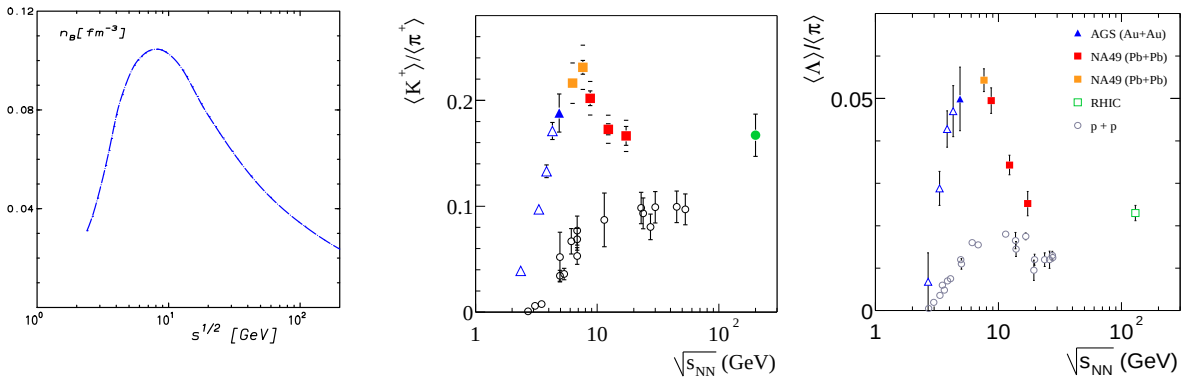

(a) (b) (c)

Figure 19: Energy dependence at freeze-out for (a) baryon density [39], (b) K^+/π^+ and (c) Λ/π^+ [41].

It is thus evident that the hadronic medium in AA collisions at freeze-out is a collective system whose properties can be accounted for by equilibrium thermodynamics, specified in terms of a temperature T and a baryochemical potential μ. It is also clear that a considerable part of the strangeness enhancement seen when comparing AA relative to pp collisions, as in Fig. 11, is due to the increase of baryon density of the medium seen by the hadronic probe. Thus it is necessary to determine what remains once this 'normal strangeness enhancement' is taken into account.

The high energy behaviour of the ratios shown in Figs. 19b and c is just the $\mu \to 0$ limit. For both cases, the corresponding results from $pp/p\bar{p}$ collsions are included. We see that nuclear collisions provide at all energies species abundances in accord with hadronization through equilibrium thermodynamics; in contrast, elementary hadron-hadron interactions lead to the mentioned 'anomalous strangeness suppression'. Thus there is no strangeness enhancement in nuclear interactions; instead, we have to understand the observed deviations from thermal behaviour in elementary hadron-hadron collisions.

The origin of this anomalous strangeness suppression is most likely due to the small density of strange particles in elementary collisions. This requires local strangeness conservation [42, 43], which suppresses strange particle production. Only for the higher strange particle densities in AA collisions, an ideal gas grand-canonical formulation becomes valid, removing the pp suppression [43]. At the same time, this shows that the medium provided by AA collisions in the hadronic stage indeed shows large scale collective behaviour.

The low mass dilepton enhancement can be understood in terms of a modification of the ρ in an interacting hadronic medium, changing its mass [44], its width [45], or both. If this modification is primarily due to interactions of the ρ with nucleons and nucleon resonances in a dense nuclear environment [45], an increase of the baryon density should increase the effect. This is indeed observed [25], suggesting that also in this case the

large baryon density of the system plays a crucial role for the observed difference between central AA and pp interactions. The behaviour of the enhancement with increasing $\sqrt{s}$ will clarify how much further thermal effects remain beyond this.

The energy dependence of hadronic probes in AA collisions in the SPS range thus provides an excellent tool to investigate the baryon density dependence of hadronization and the resulting interacting hadron system. While many hadronic variables show a change of behaviour when the baryon density starts to decrease, such studies have so far not revealed any clear threshold.

The observed photon excess constitutes a first candidate for thermal emission. Similarly, the intermediate mass dilepton enhancement has been attributed to thermal emission during the evolution of the system [46]. In both cases, more data appear necessary to identify the observed effects.

It seems not easy to reconcile the observed HBT results with an evolution of a hot thermal source. Increasing the collision energy will increase the initial energy density, and if the system is thermal in an early deconfined stage, expansion should lead to larger source sizes at higher energies. If the final source size is defined by a freeze-out condition requiring a mean free path of hadronic size [16], the baryonic composition of the hadronic medium can affect the source size, leading to a minimum of the freeze-out volume at the point of maximum baryon density [47]. The expected increase would then occur only beyond this point, as the system becomes meson-dominated. A systematic high energy study in the RHIC/LHC range will certainly clarify this. Another, rather basic question is whether an individual AA collision already produces a thermal medium, or whether only a superposition of many events leads to the observed thermal pattern.

The presence of elliptic flow can only be accounted for as consequence of the different pressure gradients in non-central interactions, and thus supports the presence of a thermal medium on an event-by-event basis. It is striking, however, that the change of elliptic flow from out-of-plane low energy to in-plane high energy behaviour (see Fig. 9) occurs essentially at the turning point of the baryon density. It thus remains to be clarified to what extent this effect is due to the nuclear medium, and how much of it persists for $\mu \to 0$.

The mass-dependent broadening of hadronic transverse momentum spectra is in accord with predictions from radial flow studies, which also assume a thermal medium per single event. Here, however, the role of initial state effects due to production from multiple scattering is not fully clarified. Hydrodynamic radial flow of an expanding thermal source would in general lead to a further increase of broadening with collision energy, while initial state effects would result in saturation. Hence a comparison between SPS and higher energy data should resolve the issue.

In summary:

- The centrality dependence of J/ψ production shows a clear onset of 'anomalous' behaviour, indicating the formation of a deconfined partonic medium.
- Species abundances and strangeness production in high energy AA collisions are in accord with ideal resonance gas thermodynamics at the confinement/deconfinement transition.

Our views today thus are clearer, but also somewhat different from what they were at the beginning of the programme. We have evidence for deconfinement as well as for thermal behaviour, but at different evolution stages. What we know now is largely due to the pioneering work of the SPS experiments. It is evident that we need more work to really reach final conclusions. It is also evident, however, that the search for critical behaviour in nuclear collisions, on the partonic as well as on the hadronic side, requires looking for onsets, and here the SPS, with its energy range and the statistics bonus of a fixed target machine, is unique. Much of the further work needed will be done at the SPS, or it will not be done at all.

Acknowledgements

It is a pleasure to thank many colleagues of the SPS Heavy Ion Programme for innumerable stimulating discussions. Particular thanks for help in the preparation of this report go to P. Braun-Munzinger, F. Karsch, C. Lourenço, K. Redlich, H.-J. Specht, J. Stachel and R. Stock.

References

[1] For a recent review, see F. Karsch and E. Laermann, *Quark-Gluon Plasma 3*, R. C. Hwa and X.-N. Wang (Eds.), World Scientific 2004, 1.

[2] T. Çelik, J. Engels and H. Satz, Phys. Lett. 129 B (1983) 323.

[3] J. Engels et al., Phys. Lett. 101B (1981) 89.

[4] L. D. McLerran and B. Svetitsky, Phys. Lett. 98B (1981) 195; J. Kuti et al., Phys. Lett. 98B (1981) 199.

[5] F. Karsch and E. Laermann, Phys. Rev. D 50 (1994) 6954.

[6] See e.g. Z. Fodor, Nucl. Phys. A715 (2003) 319c.

[7] C. R. Allton et al., Phys. Rev. D 68 (2003) 014507.

[8] J.D. Bjorken, Phys. Rev. D27 (1983) 140.

[9] E.V. Shuryak, Phys. Rep. 61 (1980) 71.

[10] K. Kajantie and H.I. Miettinen, Z. Phys. C 9 (1981) 341.

[11] T. Matsui and H. Satz, Phys. Lett. B178 (1986) 416.

[12] J.D. Bjorken, Fermilab-Pub-82/59-THY (1982) and Erratum.

[13] R. Pisarski, Phys. Lett. B110 (1982) 155.

[14] L. Van Hove, Phys. Lett. B118 (1982) 138.

[15] M. Gyulassy et al., Phys. Rev. C20 (1979) 2267.

[16] R. Stock, Annalen Phys. 48 (1991) 195.

[17] R. Hagedorn, Nuovo Cim. Suppl. 3 (1965) 147;
Nuovo Cim. 56A (1968) 1027.

[18] F. Becattini, Z. Phys. C 69 (1996) 485;
F. Becattini and U. Heinz, Z. Phys. C 76 (1997) 269;
F. Becattini et al., Phys. Rev. C 64 (2001) 024901.

[19] J. Rafelski and B. Müller, Phys. Rev. Lett. 48 (1982) 1066.

[20] S. A. Chin and A. K. Kerman, Phys. Rev. Lett. 43 (1979);
E. Witten, Phys. Rev. D30 (1984) 272.

[21] M.C. Abreu et al. (NA50), Phys. Lett. B410 (1997) 337;
M.C. Abreu et al. (NA50), Phys. Lett. B450 (1999) 456;
M.C. Abreu et al. (NA50), Phys. Lett. B477 (2000) 28.

[22] C. Baglin et al. (NA38), Phys. Lett. B220 (1989) 471;
M.C. Abreu et al. (NA50), Phys. Lett. B410 (1997) 337.

[23] G. Agakichiev et al. (CERES), Phys. Rev. Lett. 75 (1995) 1272;
G. Agakichiev et al. (CERES), Phys. Lett. B422 (1998) 405;
B. Lenkeit et al. (CERES), Nucl. Phys. A661 (1999) 23c;
J. P. Wessels et al. (CERES), Nucl. Phys. A715 (2003) 262c.

[24] N. Masera et al. (HELIOS-3), Nucl. Phys. A590 (1995) 93c.

[25] D. Adamová et al. (CERES), Phys. Rev. Lett. 91 (2003) 042301.

[26] M.M. Aggarwal et al. (WA98), Phys. Rev. Lett. 85 (2000) 3595.

[27] E. Scomparin et al. (NA50), Nucl. Phys. A610 (1996) 331c.

[28] R. Stock, Report at QM2004, Oakland/California, USA

[29] K. Fanebust et al. (NA57), J. Phys. G 28 (2002) 1607;
V. Manzari et al. (NA57), Nucl. Phys. A715 (2003) 140c.

[30] M. Weber et al. (NA52), J. Phys. G28 (2002) 1921.

[31] N. Armesto et al., Phys. Rev. Lett. 77 (1996) 3736;
M. Nardi and H. Satz, Phys. Lett. B 442 (1998) 14;
H. Satz, Nucl. Phys. A 661 (1999) 104c.

[32] L. McLerran and R. Venugopalan, Phys. Rev. D 49 (1994) 2233 and 3352;
D 50 (1994) 2225; for a recent review, see
L. McLerran, Nucl. Phys. A 702 (2002) 49.

[33] M. Asakawa and T. Hatsuda, Phys. Rev. Lett. 92 (2004) 012001;
P. Petreczky et al., Nucl. Phys. B 129&130 (2004) 596.

[34] S. Digal, S. Fortunato and H. Satz, Eur. Phys. J. C 32 (2004) 547.

[35] R. Vogt, Phys. Rept. 310 (1999) 197.

[36] J.-P. Blaizot, M. Dinh and J.-Y. Ollitrault, Phys. Rev. Lett. 85 (2000) 4012.

[37] P. Braun-Munzinger and J. Stachel, Nucl. Phys. A 606 (1996) 320 and
Nucl. Phys. A 638 (1998) 3c.

[38] Analysis of NA49 data by F. Becattini et al., Phys. Rev. C 64 (2001) 024901;
for a more recent analysis, see
P. Braun-Munzinger, K. Redlich and J. Stachel, *Quark-Gluon Plasma 3*,
R. C. Hwa and X.-N. Wang (Eds.), World Scientific Publ., Singapore 2004.

[39] J. Cleymans and K. Redlich, Phys. Rev. Lett. 81 (1998) 5284.

[40] V. Magas and H. Satz, Eur. Phys. J. C 32 (2003) 115.

[41] Compiled by R. Stock, hep-ph/0404125.

[42] R. Hagedorn, CERN Rept. 71 (1971);
E. V. Shuryak, Phys. Lett. B42 (1972) 357.

[43] S. Hamieh, K. Redlich and A. Tounsi, Phys. Lett. B 486 (2000) 61.

[44] G. E. Brown and M. Rho, Phys. Rept. 363 (2002) 85.

[45] R. Rapp and J. Wambach, Adv. Nucl. Phys. 25 (2000) 1.

[46] R. Rapp and E. Shuryak, Phys. Lett. B473 (2000) 13.

[47] D. Adamová et al. (CERES), Phys. Rev. Lett. 90 (2003) 022301.